

Supporting Information

$[\text{Me}_2\text{C}\{\text{SnCH}(\text{SiMe}_3)_2\}_2]_2$. A μ - Me_2C -bridged tetrastanna tetrahedrane

Michael Wagner,^a Michael Lutter,^a Bernhard Zobel,^a Wolf Hiller,^a Marc H. Prosenč,^b Klaus
Jurkschat*^a

^a *Lehrstuhl für Anorganische Chemie II, Technische Universität Dortmund,*

44221 Dortmund, Germany. E-mail: klaus.jurkschat@tu-dortmund.de;

Fax: +49 231 755 5048; Tel: +49 231 755 3800

^b *Physikalische Chemie, Technische Universität Kaiserslautern, Germany; DFT calculations*

Content:

1. Experimental section and NMR spectra	S2
2. Crystallography	S11
3. Computational Details	S15
4. References	S21

1. Experimental section and NMR spectra

$(RCl_2Sn)_2CMe_2$ [$R = (Me_3Si)_2CH$] and $(^{Mes}NacNacMg)_2$ were prepared as previously described.^{S1} NMR spectra were recorded on a Bruker AV DPX 300/DRX 400/DRX 500, Varian Mercury (200 MHz) or Varian Inova (500/600 MHz) instrument at room temperature. NMR chemical shifts are given in ppm and were referenced to Me_4Si or Me_4Sn (^{119}Sn). The IR spectra (cm^{-1}) were recorded on a Perkin Elmer Spectrum Two (ATR). Melting points were measured on a Büchi M-560. Elemental analyses were performed on a LECO-CHNS-932 analyzer.

Synthesis of 2,2-bis[bis(trimethylsilyl)methyldihydridostannyl]propane, $[(Me_3Si)_2(H)C(H_2)Sn]_2CMe_2$ (**2**).

To a magnetically stirred suspension of $LiAlH_4$ (1.0 g, 26.3 mmol) in Et_2O (200 mL) was added drop-wise over a period of 1 h and at 0 °C a solution of **1** (6.1 g, 8.3 mmol) in Et_2O (80 mL). The reaction mixture was warmed to room temperature and stirred for additional 12 h. The suspension thus obtained was hydrolyzed with degassed water (120 mL). The organic layer was separated, washed three times with a 20% aqueous solution of Seignette salt and dried over Na_2SO_4 . Separation of the latter by filtration and evaporation of the solvent gave 4.2 g (84%) compound **2** as colorless solid material with m.p. of 63-64 °C.

1H NMR (200.13 MHz, C_6D_6): δ -0.42 (s, 1H, $^2J(^1H-^{117/119}Sn) = 79/82$ Hz, CH), 0.18 (s, 18H, $SiCH_3$), 1.66 (s, 3H, $^3J(^1H-^{117/119}Sn) = 83/85$ Hz, CCH_3), 5.47 (s, 2H, $^1J(^1H-^{117/119}Sn) = 1632/1709$ Hz, $^3J(^1H-^{117/119}Sn) = 12$ Hz, SnH_2); $^{13}C\{^1H\}$ NMR (100.62 MHz, C_6D_6): δ -3.4 ($^1J(^{13}C-^{117/119}Sn) = 143/149$ Hz, $^1J(^{13}C-^{29}Si) = 40$ Hz, CH), 2.8 ($^1J(^{13}C-^{29}Si) = 52$ Hz, $^3J(^{13}C-^{117/119}Sn) = 17$ Hz, $SiCH_3$), 9.7 ($^1J(^{13}C-^{117/119}Sn) = 338/354$ Hz, CCH_3), 30.2 ($^2J(^{13}C-^{117/119}Sn) = 18$ Hz, CCH_3); ^{119}Sn NMR (149.2 MHz, C_6D_6 , 1H coupled): δ -138 (t of *pseudo*-octet, $^1J(^{119}Sn-^1H) = 1713$ Hz, $J(^{119}Sn-^1H) = 85$ Hz); IR (ATR): $\tilde{\nu} = 2950$ (CH), 2892 (CH), 2836 (CH), 1839 (SnH, shoulder), 1820 (SnH), 1251, 1017, 945, 831, 717, 617, 595, 486, 402; The elemental analysis showed a too low carbon content (29.65 vs. 33.9 %).

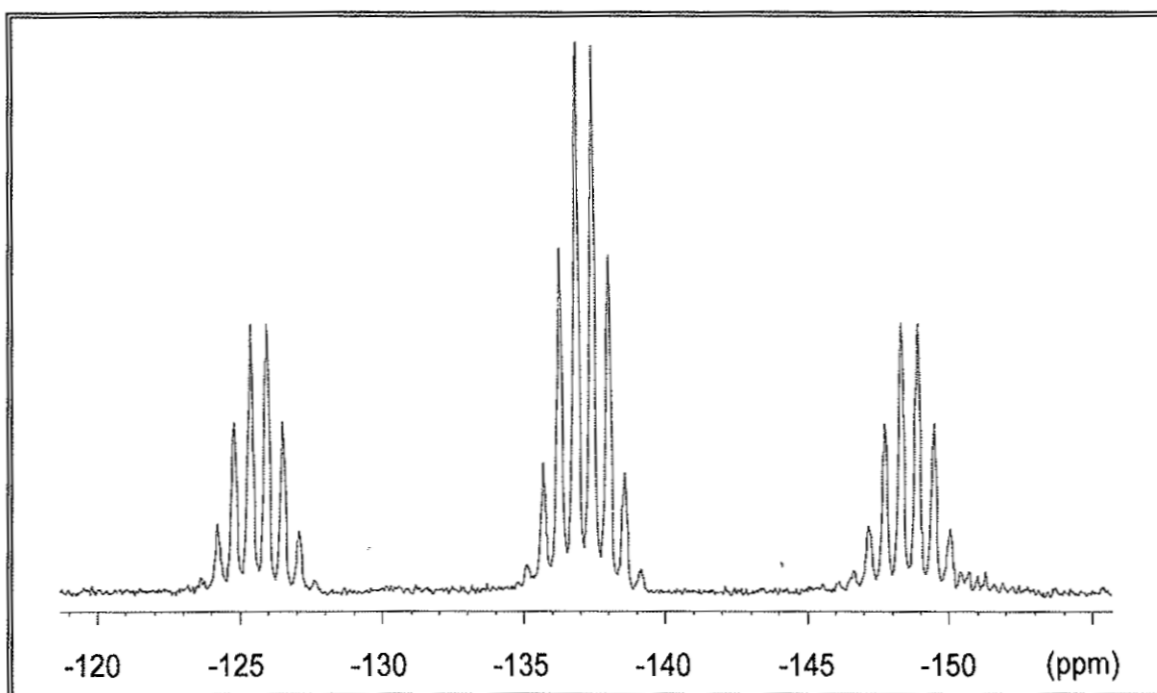


Figure S1. ^{119}Sn NMR spectrum of compound **2** (^1H coupled).^{S1a}

Synthesis of $\{[(\text{Me}_3\text{Si})_2\text{CHSn}]_2\text{CMe}_2\}_2$ (**3**).

To $(\text{RCl}_2\text{Sn})_2\text{CMe}_2$ (**1**, 174 mg, 0.236 mmol) in toluene (2 mL) was added $(^{\text{Mes}}\text{NacNacMg})_2$ (338 mg, 0.472 mmol, 2 eq) in one portion at -90°C . The suspension was warmed to room temperature and Et_2O (0.4 mL) was added. The suspension was stirred for 30 min during which the color changed to red brown. NMR spectra of the reaction mixture were recorded.

$^{29}\text{Si}\{^1\text{H}\}$ INEPT NMR (59.63 MHz, $\text{C}_6\text{D}_6/\text{toluene}/\text{ether}$): δ 0.9 (s); $^{119}\text{Sn}\{^1\text{H}\}$ NMR (111.92 MHz, $\text{C}_6\text{D}_6/\text{toluene}/\text{ether}$): δ 15 (s, $J(^{119}\text{Sn}-^{117}\text{Sn}) = 603$ Hz); $^{13}\text{C}\{^1\text{H}\}$ NMR (75.47 MHz, $\text{C}_6\text{D}_6/\text{toluene}/\text{ether}$ [solvent signals not stated]): δ 4.3 (s, SiCH_3), 10.5 (s, CH), 37.3 (s, CCH_3), 73.6 (s, CCH_3).

The solvents were removed in vacuo leaving a blue residue which was extracted with *i*-hexane giving a red suspension. The latter was filtrated. The solution was concentrated in vacuo and blue crystals suitable for X-Ray diffraction were obtained at -25°C .

In an analogues experiment using only toluene with $(^{\text{Mes}}\text{NacNacMg})_2$ (2.1 eq) added at room temperature a red oil was obtained which was dissolved in C_6D_6 and flame sealed in a NMR tube. The $^1\text{H}/^{13}\text{C}$ NMR spectra thus obtained show considerable contamination (^1H : δ 0.8-2.4, 4.8-5.0, 6.5-7.1, 12.14 ppm, ^{13}C δ 17-24, 94-96, 125-168 ppm), stemming from the reducing

agent with only one impurity unambiguously identified (δ ^1H : 12.14 ppm, $^{\text{Mes}}\text{NacNacH}$). The integral amount of the aromatic part (6.5 to 7.1 ppm) is consistent with the product containing 33% $^{\text{Mes}}\text{NacNac}$ species of diverse nature.

^1H NMR (200.13 MHz, C_6D_6): δ 0.31 (s, 72H, SiCH_3), 0.50 (s, $^2J(^1\text{H}-^{117/119}\text{Sn}) = 64$ Hz, $J(^1\text{H}-^{117/119}\text{Sn}) = 10$ Hz, 4H, CH), 2.61 (s, $^4J(^1\text{H}-^{117/119}\text{Sn}) = 21$ Hz, $^3J(^1\text{H}-^{117/119}\text{Sn}) = 76$ Hz, 12H, CCH_3); $^{13}\text{C}\{^1\text{H}\}$ NMR (100.61 MHz, C_6D_6): δ 4.3 (s, $^1J(^{13}\text{C}-^{29}\text{Si}) = 51$ Hz, SiCH_3), 10.4 (s, $^1J(^{13}\text{C}-^{29}\text{Si}) = 41$ Hz, $J(^{13}\text{C}-^{117/119}\text{Sn}) = 106$ Hz, $^1J(^{13}\text{C}-^{117/119}\text{Sn}) = 171$ Hz, CH), 37.3 (s, $^2J(^{13}\text{C}-^{117/119}\text{Sn}) = 92$ Hz, CCH_3), 73.6 (s, $^2J(^{13}\text{C}-^{117/119}\text{Sn}) = 79$ Hz, $^1J(^{13}\text{C}-^{117/119}\text{Sn}) = 101$ Hz, CCH_3); $^{29}\text{Si}\{^1\text{H}\}$ INEPT NMR (59.63 MHz, C_6D_6): δ 0.9 (s); $^{119}\text{Sn}\{^1\text{H}\}$ NMR (111.92 MHz, C_6D_6): δ 16 (s, $J(^{119}\text{Sn}-^{117}\text{Sn}) = 608$ Hz, $J(^{119}\text{Sn}-^{117}\text{Sn}) = 3289$ Hz); No elemental analysis was performed.

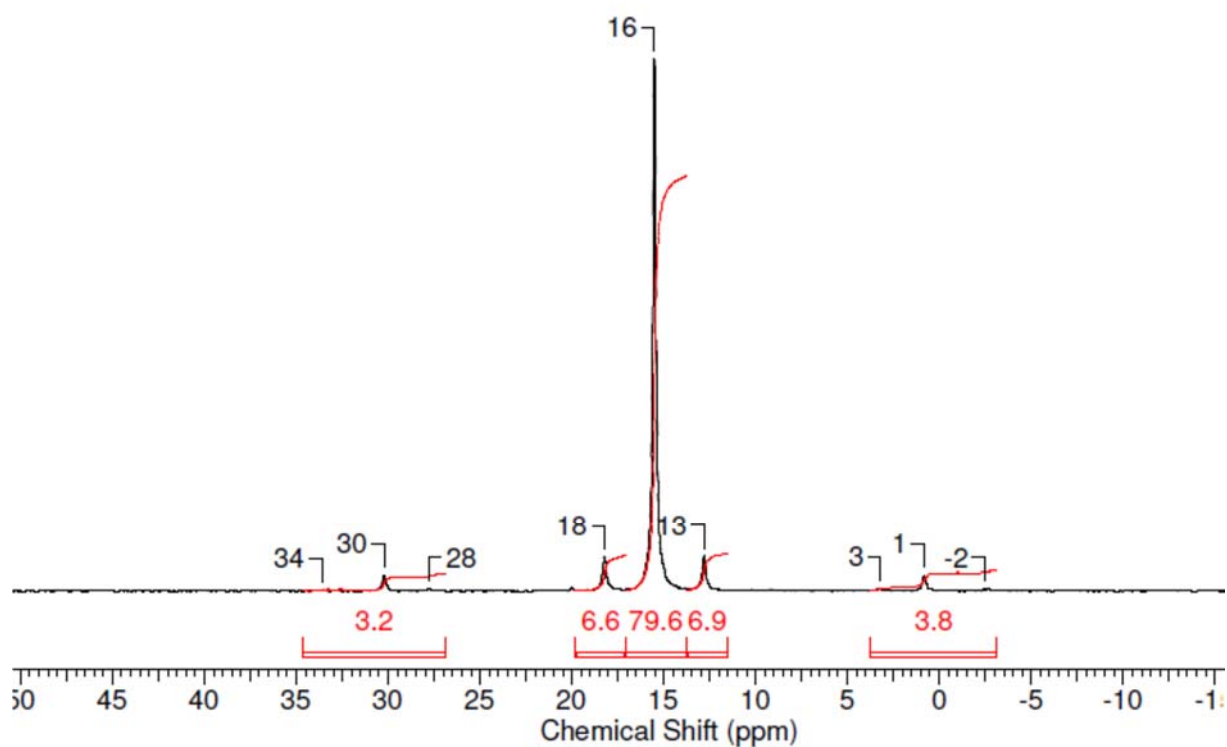


Figure S2. $^{119}\text{Sn}\{^1\text{H}\}$ NMR spectrum of compound 3 (80 k Scans).

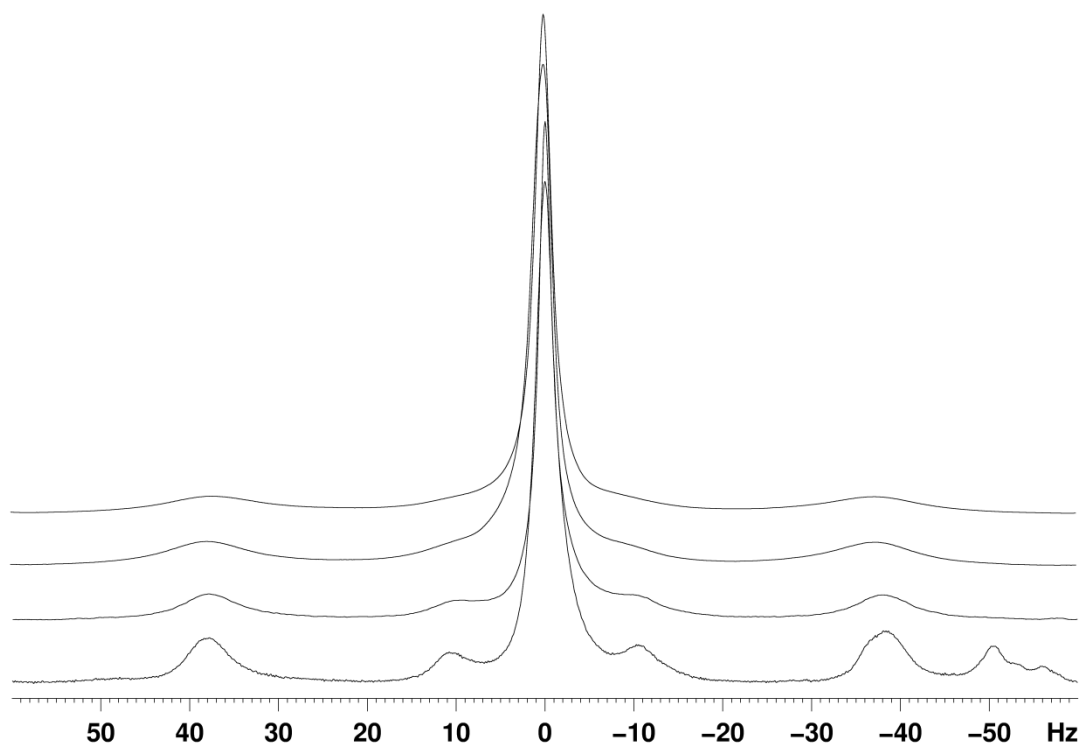


Figure S3. Superposition of the ^1H NMR spectra of the CCH_3 region at different frequencies (200, 300, 400 and 500 MHz, from bottom to top, compound **3**).

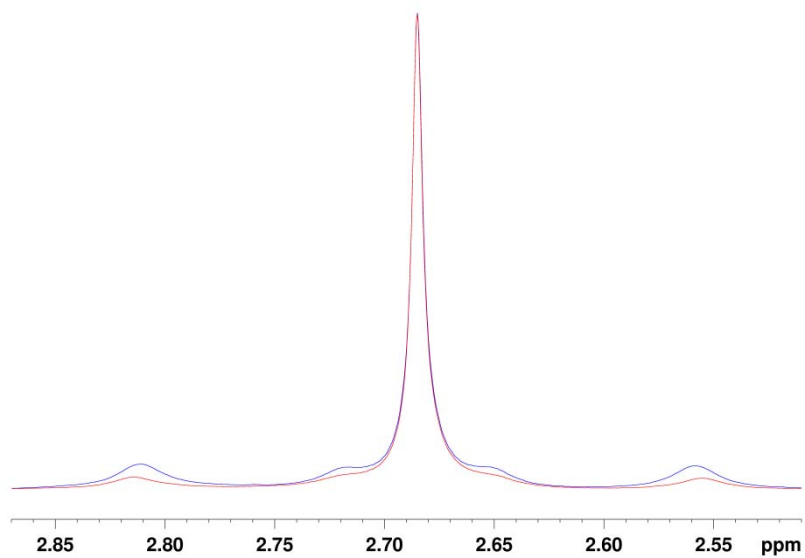


Figure S4. Superposition of the ^1H NMR spectra of the CCH_3 region with (red) and without (blue) ^{117}Sn decoupling (300 MHz) of compound **3**.

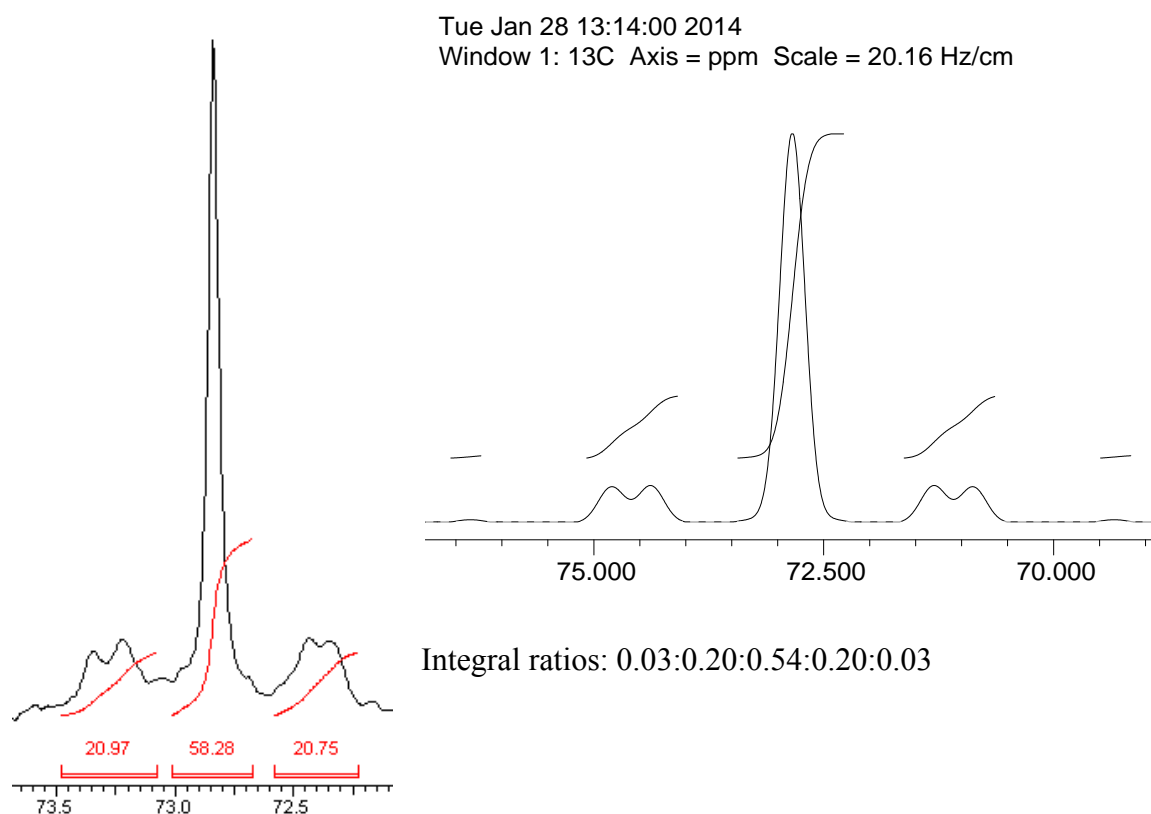


Figure S5. *left:* ^{13}C NMR spectrum of **3** (CCH_3 region, 15k Scans, processed with $\text{LB} = 5$ Hz); *right:* simulation gNMR 5.0, $^{13}\text{C}(\text{Sn1-Sn2})_2$ with $\delta = 72.84$, $W_{1/2} = 8$ Hz, $J = 101$ Hz, $J = 79$ Hz).

Time-dependent oxidation of compound **3** in C_6D_6 solution as monitored by ^{119}Sn NMR spectroscopy

The sealed NMR tube containing **3** was opened and ^{119}Sn NMR spectra were taken in time intervals.

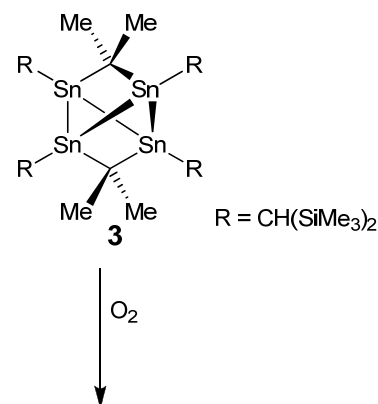
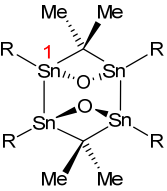
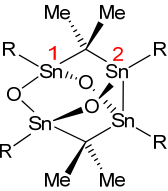
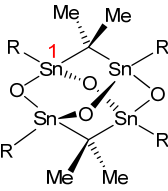


Table S1. Overview of the ¹¹⁹Sn NMR data of **4a**, **4c** and **5**

Not assigned	+ 		+ 		+ 		+ 		
	observed	expected	observed	expected	observed	expected	observed	expected	observed
20, 60 ppm (1:1) Complex coupling pattern A ¹ J(Sn-Sn) coupling constant could not be observed unambiguously.	1 signal	93 ppm	1 signal	92 ppm	2 signals (1:1)	26 (1), 81 (2) ppm	1 signal	24 ppm	
	¹ J(¹¹⁹ Sn- ¹¹⁷ Sn)	3155 Hz	¹ J(¹¹⁹ Sn- ¹¹⁷ Sn)	2840 Hz	¹ J(¹¹⁹ Sn- ¹¹⁷ Sn)	3016 Hz (2)	² J(¹¹⁹ Sn-O- ¹¹⁷ Sn)	392 Hz	
	J(¹¹⁹ Sn- ¹¹⁷ Sn)	299 Hz	J(¹¹⁹ Sn- ¹¹⁷ Sn)	285 Hz	J(¹¹⁹ Sn- ¹¹⁷ / ¹¹⁹ Sn)	100 Hz	² J(¹¹⁹ Sn-C- ¹¹⁷ Sn)	724 Hz	
	J(¹¹⁹ Sn- ¹¹⁷ Sn)	524 Hz	J(¹¹⁹ Sn- ¹¹⁷ Sn)	440 Hz	J(¹¹⁹ Sn- ¹¹⁷ / ¹¹⁹ Sn)	369 Hz			
					² J(¹¹⁹ Sn-O- ¹¹⁷ Sn)	not observed			

average values from 98/101 and 367/371 Hz; might be superimposed with the other ²J coupling of 369 Hz

From the experimental data at hand, the involvement of tin peroxides in the oxidation process cannot be ruled out.^{S3}

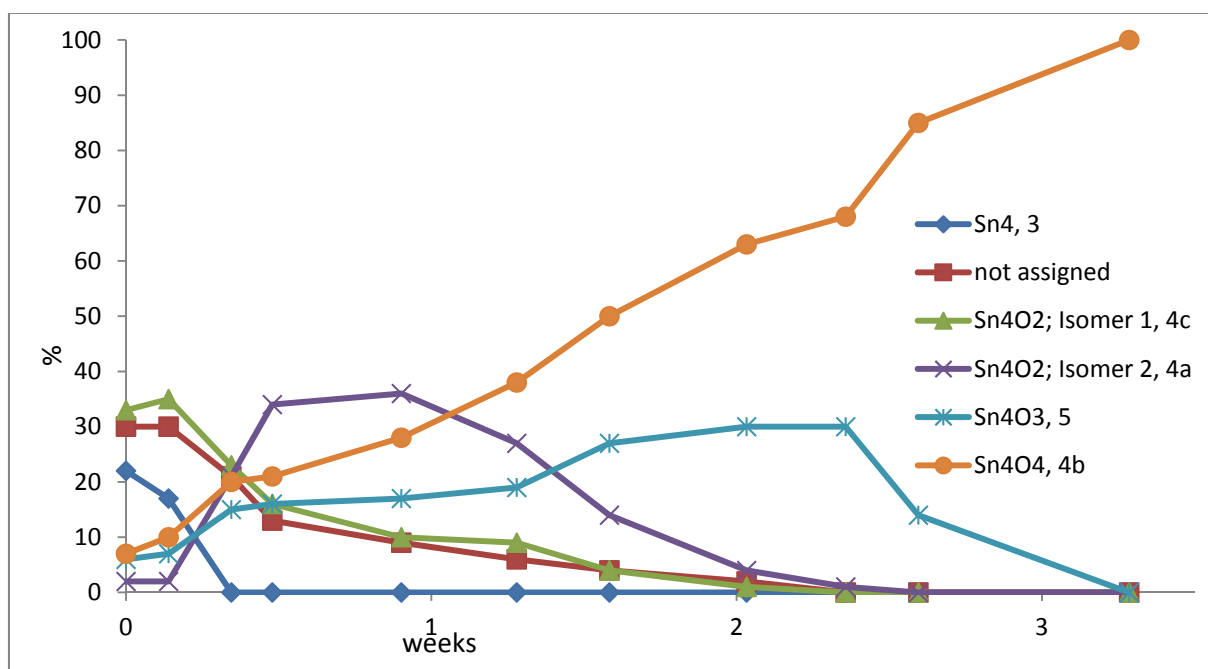


Figure S6. Plot of integral ratios from time-dependent $^{119}\text{Sn}\{^1\text{H}\}$ NMR spectra of a solution of compound **3** in C_6D_6 that had been exposed to air.

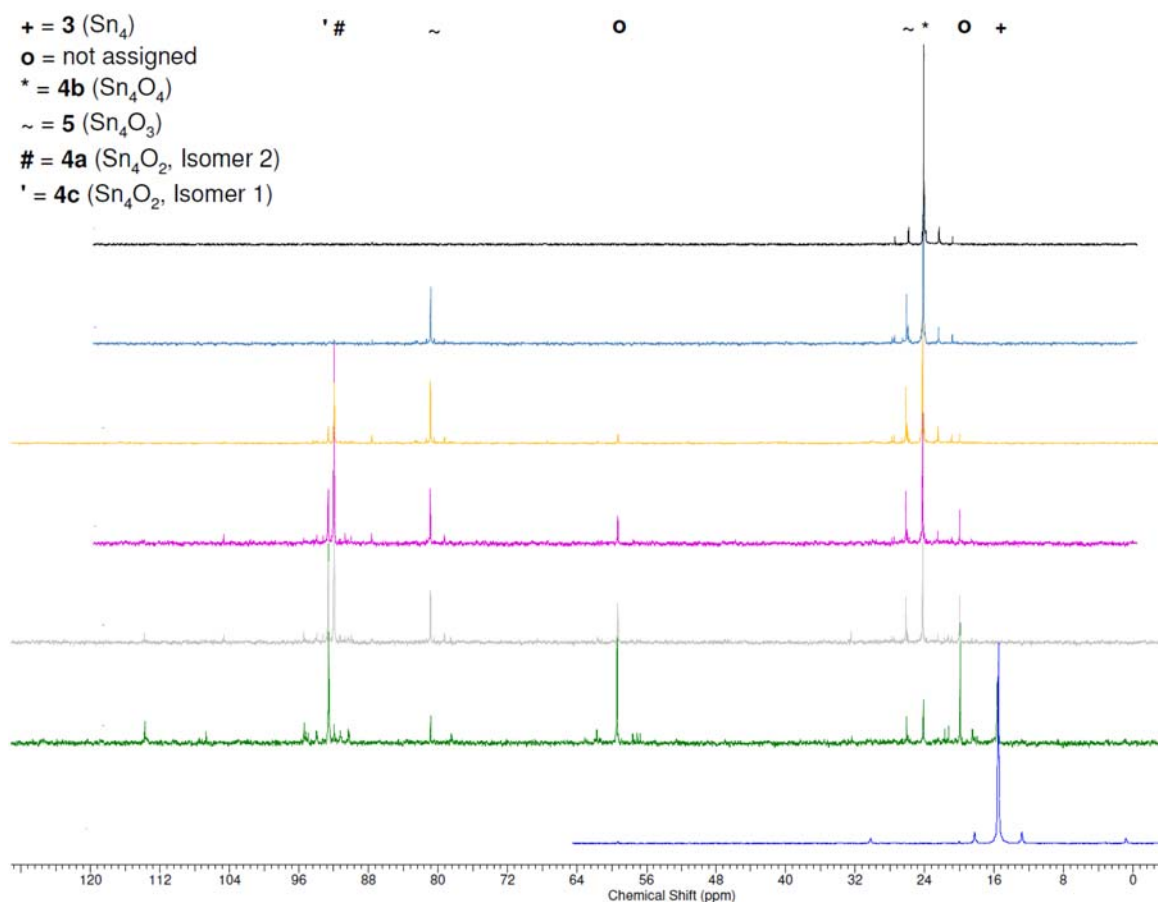
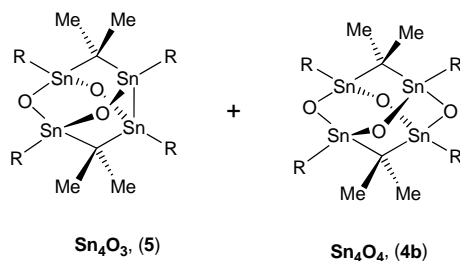


Figure S7. Time-dependent $^{119}\text{Sn}\{^1\text{H}\}$ NMR spectra of a solution of compound **3** in C_6D_6 that had been exposed to air.

NMR spectra of the three crystals that had not been analyzed by x-ray diffraction proved to be a 50:50 mixture of compound 5 and 4b:



^1H NMR (599.83 MHz, C_6D_6): δ 0.07 (s, $^2J(^1\text{H}-^{117/119}\text{Sn}) = 92$ Hz, $^2J(^1\text{H}-^{29}\text{Si}) = 8.4$ Hz, 4H, CH, **4b**), 0.12 (s, $^2J(^1\text{H}-^{117/119}\text{Sn}) = 88/92$ Hz, $^2J(^1\text{H}-^{29}\text{Si}) = 8.1$ Hz, 2H, CH, **5**), 0.26 (s, 18H, SiCH₃, **5**), 0.37 (s, 18H, SiCH₃, **5**), 0.38 (s, 72H, SiCH₃, **4b**), 0.40 (s, 36H, 2xSiCH₃, **5**), 0.54 (s, $J(^1\text{H}-^{117/119}\text{Sn}) = 27$ Hz, $^2J(^1\text{H}-^{117/119}\text{Sn}) = 88/92$ Hz, $^2J(^1\text{H}-^{29}\text{Si}) = 8.4$ Hz, 2H, CH, **5**), 1.64 (s, $^3J(^1\text{H}-^{117/119}\text{Sn}) = 94$ Hz, $^3J(^1\text{H}-^{117/119}\text{Sn}) = 110$ Hz, 6H, CCH₃, **5**), 1.74 (s, $^3J(^1\text{H}-^{117/119}\text{Sn}) = 110$ Hz, 12H, CCH₃, **4b**), 1.94 (s, $^4J(^1\text{H}-^{117/119}\text{Sn}) = 17$ Hz, $^3J(^1\text{H}-^{117/119}\text{Sn}) = 70$ Hz, $^3J(^1\text{H}-^{117/119}\text{Sn}) = 108/112$ Hz, 6H, CCH₃, **5**); $^{13}\text{C}\{^1\text{H}\}$ NMR (75.47 MHz, C_6D_6): δ 4.08 (s, SiCH₃, **5**), 4.11 (s, SiCH₃, **5**), 4.13 (s, SiCH₃, **5**), 4.15 (s, $^1J(^{13}\text{C}-^{29}\text{Si}) = 51$ Hz, $^3J(^{13}\text{C}-^{117/119}\text{Sn}) = 19$ Hz, SiCH₃, **4b**), 4.32 (s, SiCH₃, **5**), 8.77 (s, CH, **5**), 10.04 (s, CH, **5**), 10.33 (s, CH, **4b**), 23.94 (s, $^2J(^{13}\text{C}-^{117/119}\text{Sn}) = 21$ Hz [coupling found in HMBC], CCH₃, **5**), 25.62 (s, $^2J(^{13}\text{C}-^{117/119}\text{Sn}) = 15$ Hz, CCH₃, **4b**), 26.17 (s, CCH₃, **5**), 37.81 (s, CCH₃, $^1J(^{13}\text{C}-^{117/119}\text{Sn}) = 445$ Hz, $^1J(^{13}\text{C}-^{117/119}\text{Sn}) = 180$ Hz [coupling found in HMBC], **5**), 48.01 (s, CCH₃, $^1J(^{13}\text{C}-^{117/119}\text{Sn}) = 430$ Hz [coupling found in HMBC], **4b**); $^{29}\text{Si}\{^1\text{H}\}$ INEPT NMR (59.63 MHz, C_6D_6): δ 1.8 (s, $^2J(^{29}\text{Si}-^{117/119}\text{Sn}) = 34$ Hz, **5**), 1.7 (s, $^2J(^{29}\text{Si}-^{117/119}\text{Sn}) = 49$ Hz, **5**), 1.5 (s, $^2J(^{29}\text{Si}-^{117/119}\text{Sn}) = 43$ Hz, **4b**), 1.1 (s, $^2J(^{29}\text{Si}-^{117/119}\text{Sn}) = 38$ Hz, **5**), 0.3 (s, $J(^{29}\text{Si}-^{117/119}\text{Sn}) = 12$ Hz, **5**); $^{119}\text{Sn}\{^1\text{H}\}$ NMR (111.92 MHz, C_6D_6): δ 24 (s, $^2J(^{119}\text{Sn}-^{29}\text{Si}) = 45$ Hz, $^2J(^{119}\text{Sn}-\text{O}-^{117}\text{Sn}) = 392$ Hz, $^2J(^{119}\text{Sn}-\text{C}-^{117}\text{Sn}) = 742$ Hz, **4b**), 26 (s, $J(^{119}\text{Sn}-^{117/119}\text{Sn}) = 98$ Hz, $J(^{119}\text{Sn}-^{117/119}\text{Sn}) = 367$ Hz, **5**), 81 (s, $J(^{119}\text{Sn}-^{117/119}\text{Sn}) = 101$ Hz, $J(^{119}\text{Sn}-^{117/119}\text{Sn}) = 371$ Hz, **5**).

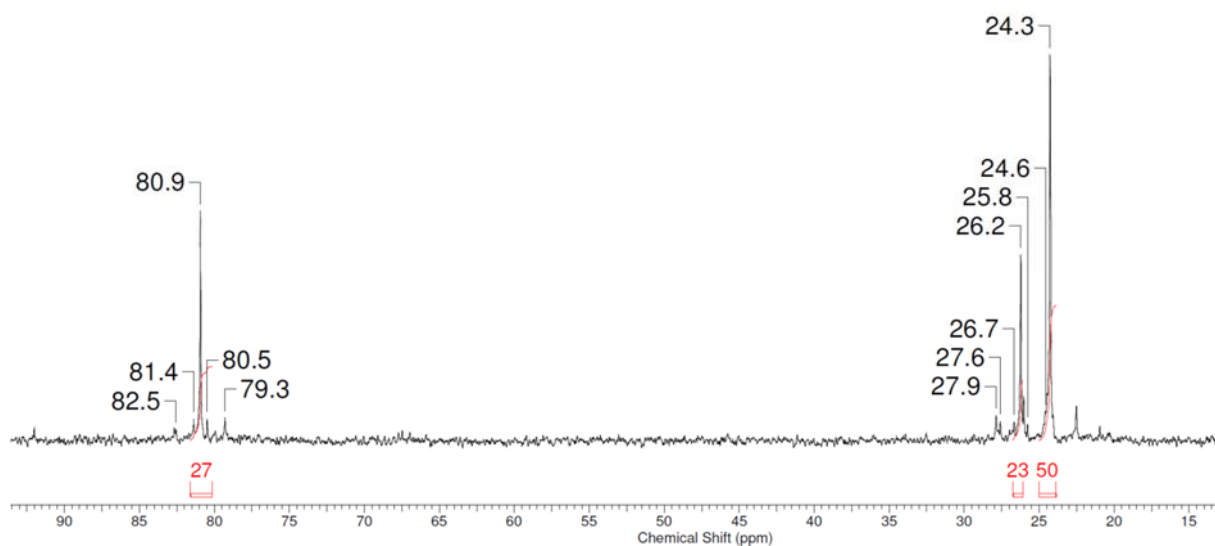


Figure S8. $^{119}\text{Sn}\{^1\text{H}\}$ NMR spectrum of a mixture of **5** (81 and 26 ppm) and **4b** (24 ppm).

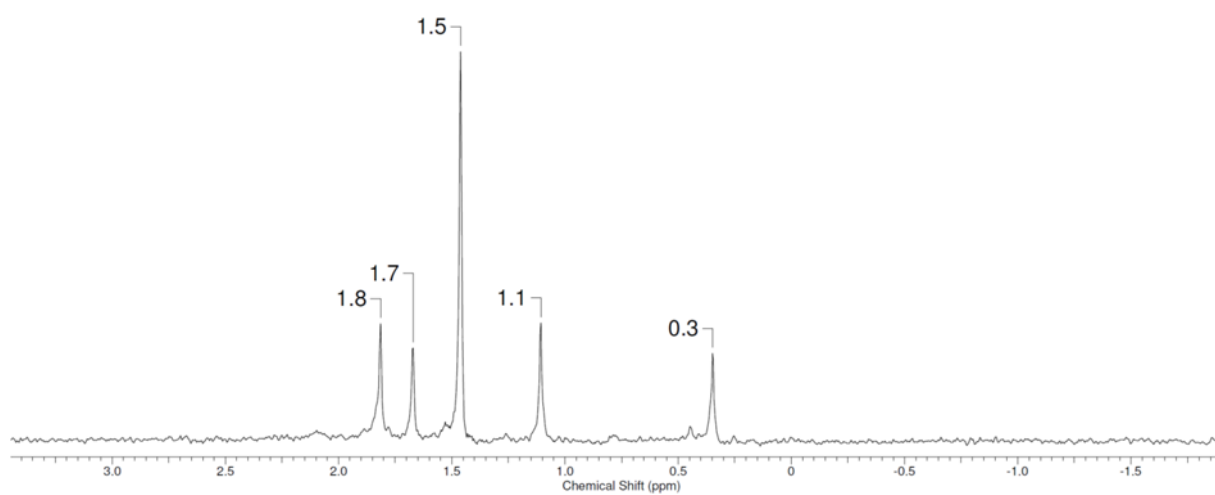


Figure S9. $^{29}\text{Si}\{^1\text{H}\}$ NMR spectrum of a mixture of **5** and **4b** (1.5 ppm).

2. Crystallography

Intensity data for the crystals (**2-4**) were collected on a XcaliburS CCD diffractometer (Oxford Diffraction) using Mo-K α radiation at 110 K. The structures were solved with direct methods using SHELXS-97.^{S4} Refinements were carried out against F^2 by using SHELXL-97.^{S4} The CH hydrogen atoms were positioned with idealized geometry and refined using a riding model, except H1 and H2 in compound **2**, which were localized in the difference Fourier map. All non-hydrogen atoms were refined using anisotropic displacement parameters. In compound **3** the carbon atom C30 is affected by disorder and was refined by a split model over two positions (occupancy values 67:33). Compound **4** is disordered between the half oxidized product and the fully oxidized product with an occupancy of 0.5 of O1. Because of changing bond lengths and bond angles between both forms, there are two refined positions for the tin atoms Sn1 and Sn2 (occupancy values 50:50). Three crystals of compound **4** were measured giving each a 50:50 disorder on free refinement. The structure of compound **4** was solved using a measurement with a detector distance of 60 mm. CCDC-1010294 (**2**), CCDC-1010295 (**3**), CCDC-1010296 (**4**) contain the supplementary crystallographic data for this paper. This data can be obtained free of charge from The Cambridge Crystallographic Data Centre via www.ccdc.cam.ac.uk/data_request/cif.

For decimal rounding of numerical parameters and su values the rules of IUCr have been employed.^{S5}

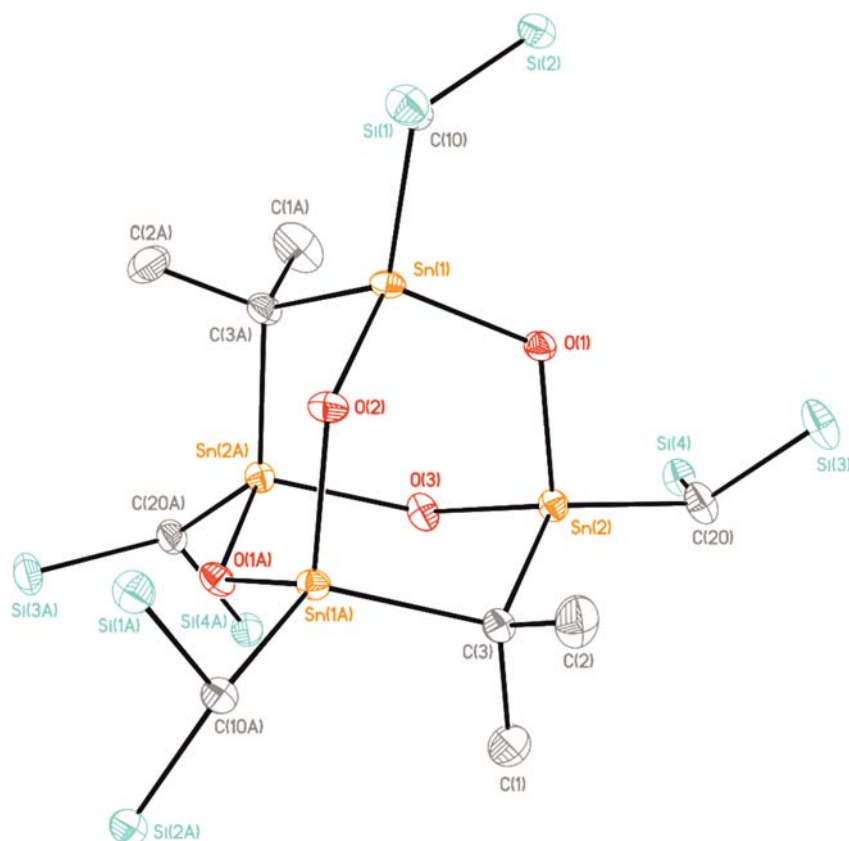


Figure S10. General view (SHELXTL) of **4b** showing 30% probability displacement ellipsoids and the atom-numbering scheme. The hydrogen atoms and methyl groups at the silicon atoms are omitted for clarity. Generation of the second half of the molecule by symmetry operation C_2 (symmetry code $-x, y, -z+1/2$). Selected interatomic distances (Å): Sn(1)–O(1) 1.962(7), Sn(2)–O(1) 1.975(4), Sn(1)–O(2) 2.001(8), Sn(2)–O(3) 2.042(3), Sn(1)–C(10) 2.049(7), Sn(1)–C(3A) 2.185(8), Sn(2)–C(3) 2.128(4), Sn(2)–C(20) 2.032(4). Selected interatomic angles (°): Sn(1)–O(1)–Sn(2) 120.4(3), Sn(1)–O(2)–Sn(1A) 125.4(4), O(1)–Sn(1)–O(2) 103.2(3), O(1)–Sn(2)–O(3) 101.45(13), C(10)–Sn(1)–C(3A) 119.5(3), C(20)–Sn(2)–C(3) 127.59(14), Sn(2)–C(3)–Sn(1A) 110.5(2).

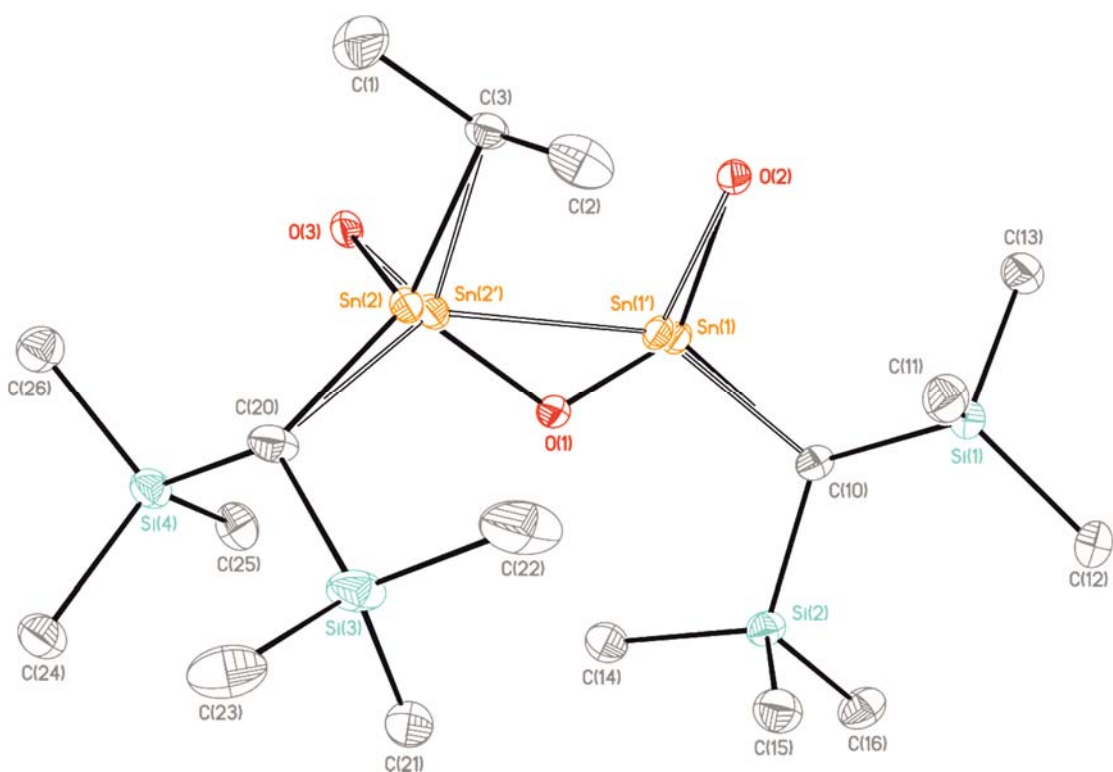


Figure S11. General view (SHELXTL) of the asymmetric unit of **4** showing 30% probability displacement ellipsoids and the atom-numbering scheme. The hydrogen atoms are omitted for clarity. Disorder tin atoms: 50:50, O(1) occupied with 50%.



Figure S12. General view (SHELXTL) of **4a/4b** showing 30% probability displacement ellipsoids and the atom-numbering scheme. The hydrogen atoms and methyl groups at the silicon atoms are omitted for clarity.

Table S2. Crystallographic data for **2-4**.

	2	3	4
Empirical formula	C ₁₇ H ₄₈ Si ₄ Sn ₂	C ₃₄ H ₈₈ Si ₈ Sn ₄	C ₃₄ H ₈₈ O ₃ Si ₈ Sn ₄
Formula mass [gmol ⁻¹]	602.29	1196.52	1244.52
λ [Å]	0.71073	0.71073	0.71073
T [K]	173(2)	173(2)	173(2)
Crystal system	monoclinic	monoclinic	monoclinic
Crystal size [mm]	0.45x0.27x0.12	0.19x0.17x0.04	0.27x0.21x0.19
Space group	<i>C2/c</i>	<i>P2₁/c</i>	<i>C2/c</i>
a [Å]	29.6997(14)	13.1495(5)	27.3250(11)
b [Å]	6.4318(3)	22.2439(7)	13.2488(4)
c [Å]	16.6792(7)	19.4674(6)	16.5435(5)
α [°]	90	90	90
β [°]	115.646(4)	103.119(4)	109.718(4)
γ [°]	90	90	90
V [Å ³]	2872.2(2)	5545.5(3)	5638.0(3)
Z	4	4	4
$\rho_{\text{calcd.}}$ [Mgm ⁻³]	1.393	1.433	1.466
μ [mm ⁻¹]	1.906	1.974	1.948
$F(000)$	1224	2416	2512
θ range [°]	2.47-25.50	2.15-25.50	2.32-25.50
Index ranges	-35 $\leq h \leq$ 35 -7 $\leq k \leq$ 7 -20 $\leq l \leq$ 20	-15 $\leq h \leq$ 11 -25 $\leq k \leq$ 26 -23 $\leq l \leq$ 23	-33 $\leq h \leq$ 32 -16 $\leq k \leq$ 16 -20 $\leq l \leq$ 20
No. of reflections collected	18036	26970	27462
Completeness of θ_{max} [%]	100.0	99.9	99.9
No. of independent reflections / R_{int}	2683 / 0.0307	10305 / 0.0367	5244 / 0.0478
No. of reflections observed with [$I > 2\sigma(I)$]	2512	8410	4551
Absorption correction	Semi-empirical from equivalents	Semi-empirical from equivalents	Semi-empirical from equivalents
$T_{\text{max}}/T_{\text{min}}$	1.0/0.79063	1.0/0.92941	1.0/0.96169
No. of refined parameters	119	451	259
GoF(F^2)	1.388	1.013	1.202
$R_1(F)$ [$I > 2\sigma(I)$]	0.0176	0.0309	0.0272
$wR_2(F^2)$ (all data)	0.0512	0.0621	0.0581
$(\Delta/\sigma)_{\text{max}}$	0.001	0.002	0.002
Largest difference peak/hole [eÅ ⁻³]	0.408 / -0.459	0.698 / -0.453	0.449 / -0.347

3. Computational Details

For all calculations on the density functional theory level, the Program RIDFT was used.^{S6} Energies and geometries were developed on the nonlocal level of theory. For geometry optimization the energies were corrected for nonlocal exchange according to Becke^{S7,8} and for nonlocal correlation according to Perdew (BP-86)^{S9} in the self-consistent procedure. The def2-TZVP-split valence base set was used for all atoms.^{S10,11} In addition, for tin atoms we used an effective core potential for inner shells (ECP-28-mwb). For the J_{ij} -term approximation an additional auxiliary base set was used.^{S2,12} All stationary points were checked by second derivative calculations revealing no imaginary frequency for the minima. NBO analyses supplied by the program was performed.^{S13}

The initial geometry was taken from X-ray structure analysis and was subsequently optimized. A second isomer was generated by rotation of one of the $\text{CH}(\text{SiMe}_3)_2$ substituents and further optimization revealed a minimum calculated to be 2 kJ lower in energy similarly to the observed disorder in compound **3**.

Calculation of Sn NMR shifts

For all DFT calculations the program system TURBOMOLE has been employed using the B3LYP functional and the def2-TZVP basis set for all atoms. Calculations of chemical shifts on organometallic Sn-containing compounds were successfully employed by Harris and Fischer.^{S14} Following their report calculations of the chemical shifts on compounds **3** and the isomeric distannene were performed employing the GIAO-algorithm within the program MPSHIFT on optimized geometries.^{S15} For the Sn-atoms an all electron TZVPall basis set^{S14,S16} was used. The calculated absolute isotropic shifts were referenced relative to the chemical shifts calculated for tetramethyltin (2579 ppm) using the same method and basis set.

From the optimized geometry of compound **3** four chemically different Sn atoms were found which is in accord with data from crystal structure analysis. The chemical shifts for these Sn-atoms range from (2433 to 2635 ppm absolute) resulting in an average shift of -65 ppm which is in the range of the observed chemical shift of 16 ppm. For a symmetrized structure (D_{2d}) the isotropic shifts were calculated to be -44 ppm. For a putative six-membered ring (distannene) the average chemical shift was calculated to be -800 ppm for the Sn-atoms which is far away from the experimentally observed shift and cannot be assigned to a distannene structure based on these calculations.

Table S3. Selected geometric parameters for optimized **3**. Angles in $^{\circ}$, distances in \AA .

Sn(1)-Sn(2)	3.315	Sn1-C(10)	2.262
Sn(2)-Sn(3)	2.943	Sn2-C(20)	2.255
Sn(3)-Sn(4)	3.276	Sn3-C(30)	2.245
Sn(4)-Sn(1)	2.965	Sn4-C(40)	2.254
Sn(1)-Sn(3)	2.917	Sn(2)-C(1)	2.272
Sn(2)-Sn(4)	2.938	Sn(4)-C(4)	2.271
Sn(1)-C(1)	2.260	Sn(3)-C(4)	2.273
Sn(1)-C(1)-Sn(2)	94.0	Sn(3)-C(2)-Sn(4)	92.2
Sn(2)-Sn(4)-Sn(1)	68.3	Sn(1)-Sn(3)-Sn(4)	56.9
Sn(3)-Sn(1)-Sn(4)	67.7	Sn(1)-Sn(4)-Sn(3)	55.5
Sn(2)-Sn(1)-Sn(4)	55.4	C(10)-Sn(1)-Sn(2)	154.2

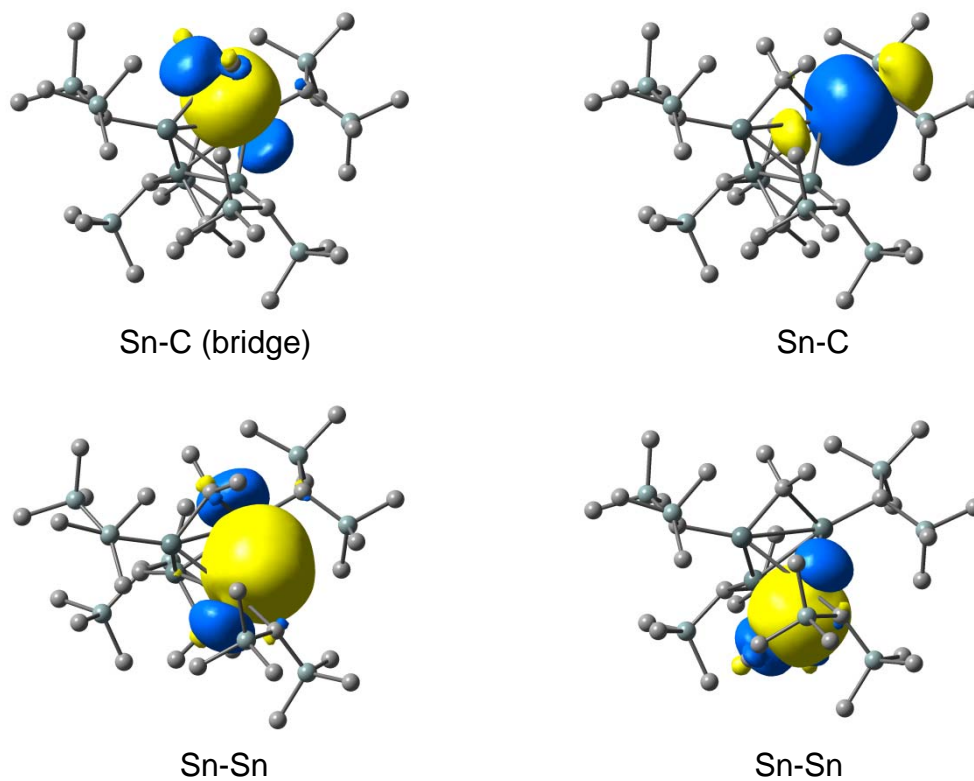


Figure S13. Natural Bonding Orbitals around selected Sn-atoms for compound **3**.

Calculations of electronic excited states^{S17} were performed on the optimized ground state structure of **3**. Electronic transitions were assigned by the corresponding Natural Transition Orbitals (see Figure S15).^{S18} The lowest energy excitations consist of an excitation from Sn-Sn bond orbitals into a cluster-Sn orbital (420 nm), from a combination of Sn-C and Sn-Sn cluster orbitals into a σ^* Sn-C cluster orbital (411 nm) and from Sn-Sn bond orbitals into σ^* Sn-C cluster orbitals (393 nm).

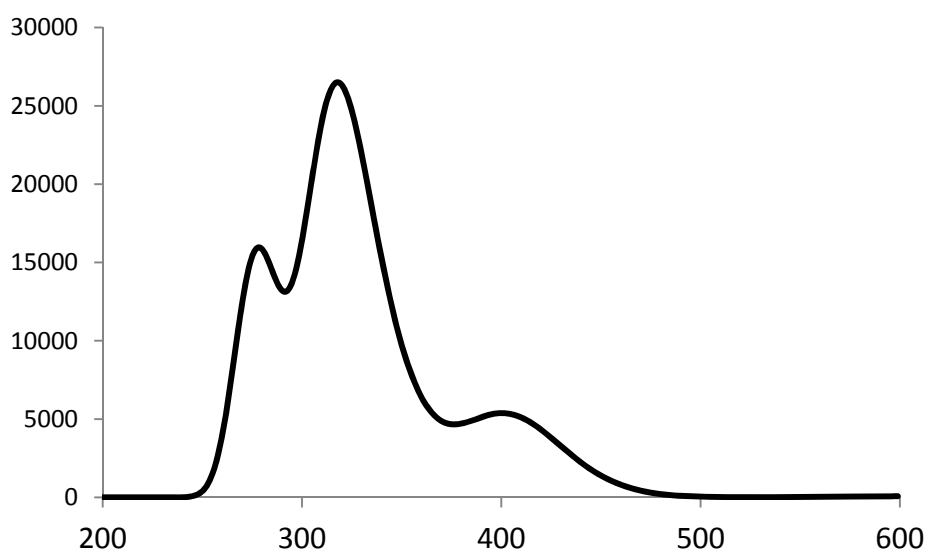


Figure S14. Calculated electronic excitation spectrum of compound **3**.

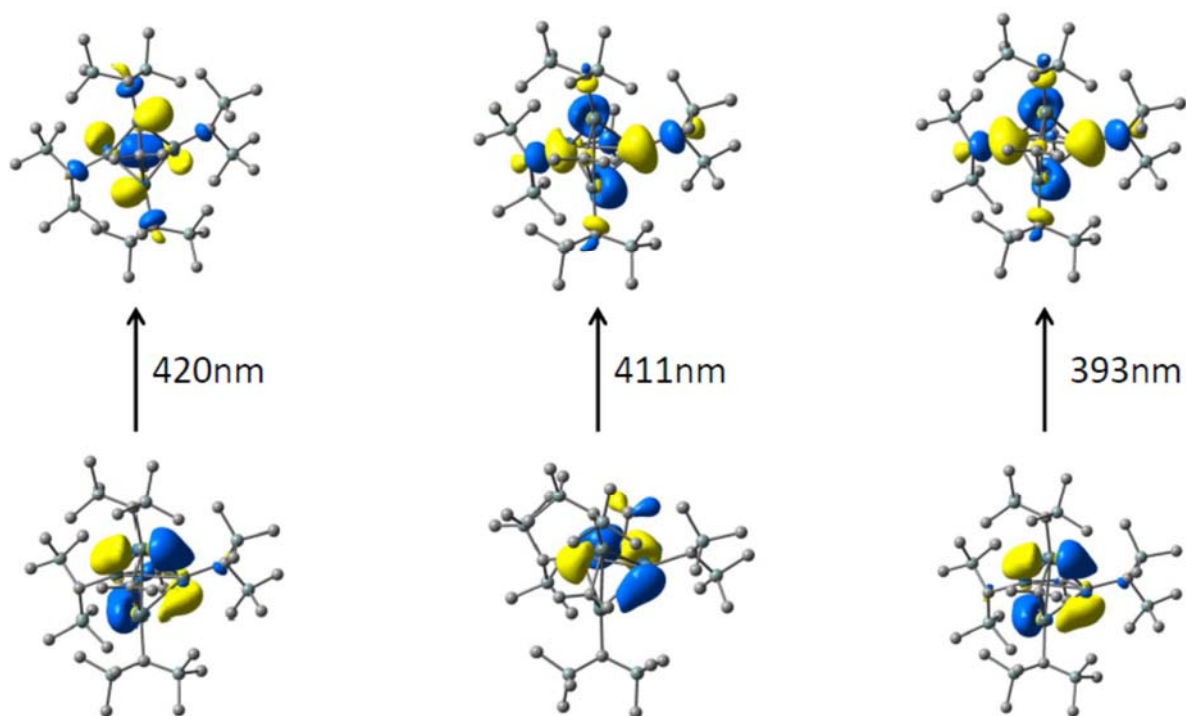


Figure S15. Natural transition orbitals for low energy excitations.

Table S4. Selected geometric parameters for optimized **4a**. Angles in °, distances in Å.

Sn(1)-Sn(2)	3.426	Sn(1)-C(10)	2.229
Sn(2)-Sn(3)	2.932	Sn(2)-C(20)	2.221
Sn(3)-Sn(4)	3.426	Sn(3)-C(30)	2.225
Sn(4)-Sn(1)	2.975	Sn(4)-C(40)	2.231
Sn(1)-Sn(3)	3.407	Sn(2)-C(1)	2.256
Sn(2)-Sn(4)	3.385	Sn(4)-C(4)	2.260
Sn(1)-C(1)	2.244	Sn(1)-O(1)	2.027
Sn(3)-C(4)	2.261	Sn(3)-O(1)	2.016
Sn(4)-O(2)	2.024	Sn(2)-O(2)	2.034
<hr/>			
C(20)-Sn(2)-Sn(1)	149.0	Sn(2)-Sn(4)-Sn(3)	51.0
C(40)-Sn(4)-Sn(3)	161.6		
Sn(1)-Sn(2)-Sn(3)	64.3	Sn(1)-O(1)-Sn(3)	114.9
Sn(1)-Sn(2)-Sn(4)	51.8	Sn(2)-O(2)-Sn(4)	113.1
Sn(2)-Sn(3)-Sn(4)	63.8	Sn(3)-C(4)-Sn(4)	98.5
Sn(2)-Sn(1)-Sn(3)	50.8	Sn(1)-C(1)-Sn(2)	99.2
Sn(3)-Sn(2)-Sn(4)	65.2		
Sn(1)-Sn(3)-Sn(2)	64.9	C(20)-Sn(2)-Sn(3)	143.9
C(10)-Sn(1)-Sn(2)	159.1	C(40)-Sn(4)-Sn(3)	161.6
C(30)-Sn(3)-Sn(4)	132.5	Sn(1)-C(1)-Sn(2)	99.1

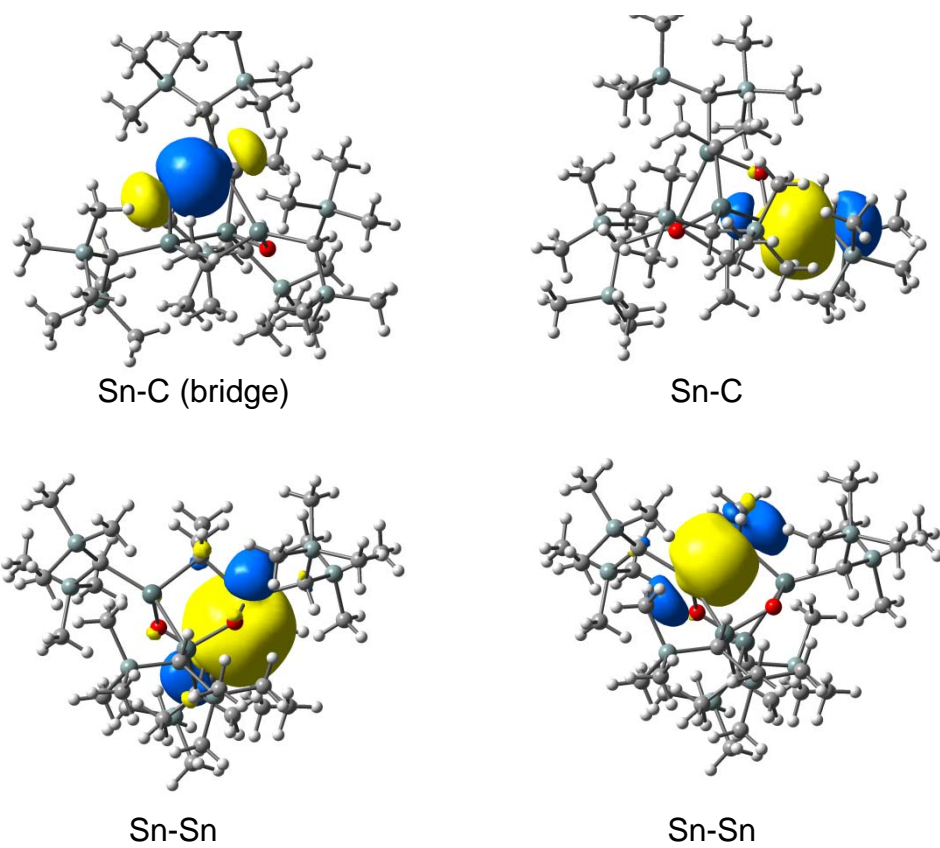


Figure S16. Natural Bonding Orbitals around selected Sn-atoms for compound **4a**.

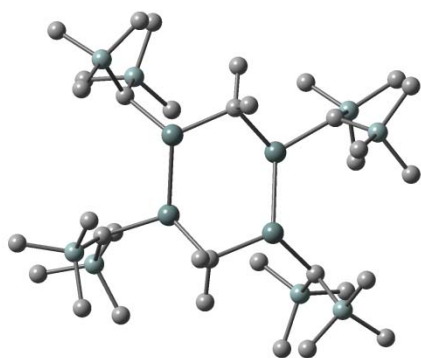


Figure S17. Calculated structure of a putative Sn₄-six membered ring.

From DFT calculations employing the same methods as stated in the manuscript, the energy calculated for the six-membered ring (distannene) is 73 kJ/mol higher than that of the Sn₄-tetrahedron.

Selected distances (Å) for the putative Sn₄-six membered ring

Sn-Sn 2.853

Sn-Sn 2.811

Sn...Sn 3.577

Sn...Sn 3.601

Sn-C(Me₂) 2.277

Sn-C(Me₂) 2.252

Sn-C(Me₂) 2.281

Sn-C(Me₂) 2.237

Sn-C 2.266

Sn-C 2.246

Sn-C 2.277

Sn-C 2.250

4. References

- S1 (a) B. Zobel, Dissertation, **1998**, Universität Dortmund; (b) B. Zobel, M. Schürmann, K. Jurkschat, D. Dakternieks, A. Duthie, *Organometallics*, 1998, **17**, 4096; (c) S. J. Bonyhady, C. Jones, S. Nembenna, A. Stasch, A. J. Edwards, G. J. McIntyre, *Chem. Eur. J.*, 2010, **16**, 938.
- S2 gNMR 5.0.6.0 (P. H. M. Budzelaar, Ivory Soft), **2006**.
- S3 (a) J. J. Schneider, J. Hagen, O. Heinemann, J. Bruckmann, C. Krüger, *Thin Solid Films*, 1997, **304**, 144; (b) C. J. Cardin, D. J. Cardin, M. M. Devereux, M. A. Convery, *J. Chem. Soc., Chem. Commun.*, 1990, 1461; (c) R. W. Chorley, P. B. Hitchcock, M. F. Lappert, *J. Chem. Soc., Chem. Commun.*, 1992, 525.
- S4 G. M. Sheldrick, *Acta Cryst.*, 2008, **A64**, 112.
- S5 W. Clegg, *Acta Cryst.*, 2003, **E59**, 2.
- S6 K. Eichkorn, O. Treutler, H. Öhm, M. Häser, R. Ahlrichs, *Chem. Phys. Lett.*, 1995, **242**, 652.
- S7 (a) A. D. Becke, *J. Chem. Phys.*, 1986, **84**, 4524; (b) A. D. Becke, *J. Chem. Phys.*, 1988, **88**, 1053.
- S8 A. D. Becke, *Phys. Rev. A*, 1988, **38**, 3098.
- S9 (a) J. P. Perdew, *Phys. Rev.*, 1986, **B33**, 8822; (b) J. P. Perdew, *Phys. Rev.*, 1986, **B34**, 7406.
- S10 R. Ahlrichs, M. Bär, M. Häser, H. Horn, C. Kölmel, *Chem. Phys. Lett.*, 1989, **162**, 165.
- S11 M. Häser, R. Ahlrichs, *J. Comp. Chem.*, 1989, **10**, 104.
- S12 B. I. Dunlap, J. W. D. Connolly, J. R. Sabin, *J. Chem. Phys.*, 1979, **71**, 339.
- S13 (a) J. P. Foster, F. Weinhold, *J. Am. Chem. Soc.*, 1980, **102**, 7211; (b) F. Weinhold, C. R. Landis, *Valency and Bonding: A Natural Bond Orbital Donor-Acceptor Perspective*,

Cambridge University Press, 2005; (c) A. E. Reed, L. A. Curtiss, F. Weinhold, *Chem. Rev.*, 1988, **88**, 899.

S14 P. Avalle, R. K. Harris, R. D. Fischer, *Phys. Chem. Chem. Phys.*, 2002, **4**, 3558.

S15 (a) M. Kollwitz, J. Gauss, *Chem. Phys. Lett.*, 1996, **260**, 639; (b) M. Kollwitz, M. Häser, J. Gauss, *J. Chem. Phys.*, 1998, **108**, 8295; (c) U. Huniar, Dissertation, 1999, Universität Karlsruhe.

S16 R. Ahlrichs, K. May, *Phys. Chem. Chem. Phys.*, 2000, **2**, 943.

S17 R. Bauernschmitt, R. Ahlrichs, *Chem. Phys. Lett.*, 1996, **256**, 454–464.

S18 R. L. Martin, *J. Chem. Phys.*, 2003, **118**, 4775.